



An Updated 2017 Astrometric Solution for Betelgeuse

G. M. Harper¹, A. Brown¹, E. F. Guinan², E. O’Gorman³, A. M. S. Richards⁴, P. Kervella^{5,6}, and L. Decin⁷

¹Center for Astrophysics and Space Astronomy, University of Colorado,
Boulder, CO 80309, USA; graham.harper@colorado.edu

²Villanova University, 800 Lancaster Avenue, Villanova, PA 19085, USA

³Dublin Institute for Advanced Studies, 31 Fitzwilliam Place, Dublin 2, D02 XF86, Ireland

⁴Jodrell Bank Centre for Astrophysics, School of Physics and Astronomy, University of Manchester, UK

⁵Unidad Mixta Internacional Franco-Chilena de Astronomía (UMI 3386),
Departamento de Astronomía, Universidad de Chile, Santiago, Chile

⁶Observatoire de Paris, PSL Research University, CNRS, UPMC, Univ. Paris-Diderot, France

⁷Instituut voor Sterrenkunde, Katholieke Universiteit Leuven, Celestijnenlaan 200D, 3001 Leuven, Belgium

Received 2017 April 10; accepted 2017 April 25; published 2017 June 16

Abstract

We provide an update for the astrometric solution for the Type II supernova progenitor Betelgeuse using the revised *Hipparcos* Intermediate Astrometric Data (HIAD) of van Leeuwen, combined with existing VLA and new e-MERLIN and ALMA positions. The 2007 *Hipparcos* refined abscissa measurements required the addition of so-called *Cosmic Noise* of 2.4 mas to find an acceptable 5-parameter stochastic solution. We find that a measure of radio *Cosmic Noise* should also be included for the radio positions because surface inhomogeneities exist at a level significant enough to introduce additional intensity centroid uncertainty. Combining the 2007 HIAD with the proper motions based solely on the radio positions leads to a parallax of $\pi = 5.27 \pm 0.78$ mas (190_{-25}^{+33} pc), smaller than the *Hipparcos* 2007 value of 6.56 ± 0.83 mas (152_{-17}^{+22} pc). Furthermore, combining the VLA and new e-MERLIN and ALMA radio positions with the 2007 HIAD, and including radio *Cosmic Noise* of 2.4 mas, leads to a nominal parallax solution of 4.51 ± 0.80 mas (222_{-34}^{+48} pc), which, while only 0.7σ different from the 2008 solution of Harper et al., is 2.6σ different from the solution of van Leeuwen. An accurate and precise parallax for Betelgeuse is always going to be difficult to obtain because it is small compared to the stellar angular diameter ($\theta = 44$ mas). We outline an observing strategy utilizing future mm and sub-mm high-spatial resolution interferometry that must be used if substantial improvements in the precision and accuracy of the parallax and distance are to be achieved.

Key words: astrometry – stars: distances – stars: fundamental parameters – stars: individual (α Ori) – stars: massive – radio continuum: stars

1. Introduction

The parallax of the red supergiant Betelgeuse (α Ori: M2 Iab) is of considerable interest to the astrophysics community because it is required to determine the fundamental stellar parameters and to constrain its evolutionary status, e.g., an age of ~ 8 – 10 Myr, with < 1 Myr until it explodes (Harper et al. 2008; Dolan et al. 2016). There is a paucity of M supergiants in the solar neighborhood, and Betelgeuse is one of only two nearby supernova progenitors—the other being Antares (M1 Iab + B3 V: dist $\simeq 200$ pc). If Betelgeuse explodes as a red supergiant, Betelgeuse will likely become a Type II-P, or if it evolves blueward, it may become a Type II-L (see Smith et al. 2009). As a bright large angular diameter source it has been the focus of innumerable multi-wavelength observational studies, but relatively few theoretical ones. It is frustrating that its parallax is currently so poorly constrained: $5.07 \pm 1.10(1\sigma)$ mas (197_{-35}^{+55} pc; Harper et al. 2008), which severely limits what can be gleaned from all of the research effort into this system. The luminosity reflects the star’s mass and, hence, its evolution and lifetime, and with its interferometric angular diameter of $\simeq 44$ mas (e.g., Haubois et al. 2009; Ohnaka et al. 2009; Montargès et al. 2016), a direct estimate of the surface gravity can be obtained. Accurate stellar parameters are also crucial to limit the parameter space of theoretical and numerical studies of stellar structure (e.g., Freytag et al. 2002), mass loss mechanism (Hartmann & Avrett 1984; Airapetian et al. 2000), and circumstellar structure (Harper et al. 2017).

The inherent problem for astrometric solutions for stars with angular diameters larger than their parallax is that any deviation of the center of intensity from the center-of-mass (CoM or barycenter) leads to additional systematic uncertainties. Both Betelgeuse and Antares (α Sco: M1 Iab) have angular diameters, $\simeq 44$ mas, and distances near 200 pc, and their parallaxes are $\simeq 5$ mas. The release of the original *Hipparcos* catalog (ESA 1997; Perryman et al. 1997) suggested that Betelgeuse had a distance of 131_{-23}^{+35} pc, closer than many other astrophysical estimates, (see Harper et al. 2008, and references therein). That astrometric solution required the addition of 3.4 ± 0.6 mas of *Cosmic Noise*⁸ to obtain a stochastic 5-parameter astrometric solution (i.e., R.A. (α), decl. (δ), parallax (π), and proper motions in $\alpha \cos \delta$ and δ). The specific origin of this additional positional uncertainty remains unknown: potential origins include source size, brightness and photon counting saturation (see ESA 1997), and movement of the stellar photo-center, which may result from large-scale convective/pulsation-induced motions in the outer layer of the star (e.g., Freytag et al. 2002). Boboltz et al. (2007) derived somewhat different proper motions to the 1997 *Hipparcos* solution, and this was confirmed by subsequent multi-wavelength VLA cm-radio interferometry (Harper et al. 2008). This latter study combined VLA radio positions with the 1997 HIAD and

⁸ A stochastic solution is one in which the dispersion of the abscissa residuals about the optimum solution was greater than expected and an additional source of *Cosmic Noise* (or *Dispersion*) was added to the residual uncertainties.

Table 1
New ICRS Radio Positions for Betelgeuse

Date	R.A. (h m s)	Decl. ($^{\circ}$ ' ")	Unc. (mas)	Reference
2012.530	05 55 10.32672	07 24 25.5263	17.5	5.75 GHz, Richards et al. (2013)
2015.178	05 55 10.32882	07 24 25.5501	22.2	5.75 GHz, New
2015.422	05 55 10.32913	07 24 25.5853	22.5	5.75 GHz, New
2015.854	05 55 10.33142	07 24 25.5646	2.0	330–345 GHz ALMA
2016.623	05 55 10.33560	07 24 25.5482	14.1	330–345 GHz ALMA

found a greater distance (197_{-35}^{+55} pc) and also revealed a tension whereby the radio positions alone suggested a greater distance.

Just at the completion of the Harper et al. (2008) study, revised *Hipparcos* astrometry was published by van Leeuwen (2007; hereafter referred to as the 2007 *Hipparcos* solution). The astrometric solutions from this impressive re-analysis are generally of significantly improved quality compared to the 1997 release, and the number of single star astrometric solutions requiring *Cosmic Noise* was reduced from 1561 to 588. Betelgeuse’s revised *Hipparcos* parallax put it at 152 ± 20 pc, but the solution still required 2.4 mas of *Cosmic Noise*. Note that Antares also required 3.6 mas of *Cosmic Noise*. Recalling that the parallax derived by Harper et al. (2008) was based on the combination of VLA radio positions and the *Hipparcos* Intermediate Astrometric Data (HIAD, ESA 1997; Perryman et al. 1997), we have been asked whether the revised van Leeuwen (2007) intermediate astrometric data would lead to a different VLA+*Hipparcos* combined solution. Here, we address this question and provide updated astrometric solutions.

The importance of the radio positions for the astrometric solution is the long timeline that they provide when compared to the *Hipparcos* mission. While *Hipparcos* observed the sky for 3.2 years, Betelgeuse was observed for less than 28 months. In contrast, the radio timeline now extends from 1982 to 2016 ($\Delta t = 34$ years), and since 2008, Betelgeuse has also been observed with e-MERLIN (Garrington & Beswick 2016) by Richards et al. (2013) and ALMA. The yearly proper motions of Betelgeuse are $\simeq 10\text{--}25$ mas yr $^{-1}$, which is a significant fraction of the angular diameter per year, so the long timeline helps to define the proper-motion elements of the astrometric solution even with modest measurement uncertainties.

In Section 2, we present the new radio positions, discuss the magnitude of expected *Cosmic Noise* for the radio positions, and derive radio-only proper motions. In Section 3, we give the combined radio and 2007 *Hipparcos* astrometric solutions, and in Section 4, we discuss what is needed to find a significantly improved parallax for Betelgeuse. Conclusions are given in Section 5.

2. New Radio Positions

The new radio positions, which consist of two ALMA observations at 330–345 GHz and three e-MERLIN observations obtained at 5.75 GHz (5.2 cm) (Richards et al. 2013), are given in Table 1.

2.1. ALMA

Betelgeuse was observed by ALMA in a long baseline configuration on 2015 November 9 and again on 2016 August 16 in a more compact configuration (Project code: 2015.1.00206.S, PI: P. Kervella). Both sets of observations were carried out in Band 7 with identical spectral setups and will be described in more detail

in a future publication (P. Kervella et al. 2017, in preparation). For the purpose of this work, the channels containing line emission were excluded from the analysis and a single continuum data set centered at $\simeq 338$ GHz with a ~ 5.9 GHz bandwidth was used. The maximum baseline in the long baseline observation was 16 km, which yielded an angular resolution of ~ 15 mas, while the maximum baseline provided by the more compact configuration observation was 1.2 km, which yielded an angular resolution of 185 mas. The observations of Betelgeuse (Star) were interleaved with observations of the compact phase calibrator J0552+0313 (PhaseCal) located approximately 4 deg away from the target using a 2-min cycle time. The compact source J0605+0939 (ChkSource), located approximately 7 deg from the PhaseCal, was used as a check source. ChkSource was found to be located 3.3 mas away from its expected position. For the compact configuration, the same phase calibrator (J0552+0313) was again used, but a longer cycle time of 7.5 minutes was implemented. J0603+0622 was used as a check source and was found to be located 15 mas away from its expected position. For both epochs, the source position was extracted from the un-self-calibrated continuum data sets using the Python-based task *uvmultifit* (Martí-Vidal et al. 2014) and fitting a uniform intensity elliptical disk to the calibrated visibilities.

The positional uncertainties (Unc) for the two Betelgeuse observations are dominated by the phase-referencing uncertainty (and not fit errors). We used the difference between the measured positions of ChkSource from those expected, ΔCS , scaled by the relative separation of Star and PhaseCal, and the ChkSource and PhaseCal, i.e.,

$$\text{Unc} = \Delta CS \times (\text{Star} - \text{PhaseCal}) / (\text{ChkSource} - \text{PhaseCal}).$$

These uncertainties for the ALMA positions are given in Table 2. During the compact configuration observation, the wind speed was high and increased during the observations, which increased the atmospheric instability. This in turn might lead to an underestimation of the uncertainty reported in Table 2.

2.2. e-MERLIN

Betelgeuse was observed in the first semester of e-MERLIN open time in 2012 July, with a bandwidth of 512 MHz centered on 5.75 GHz (5.2 cm). Seven antennas were used, including the 75 m Lovell telescope, providing baselines from 11 to 217 km (90–3910 k λ). The data were processed in dual polarization, using 4×128 MHz spectral windows, each divided into 64×2 MHz channels.

The point-like QSO 0551+0829, separation $\sim 1^{\circ}.5$, was used as the phase reference on a cycle of 7:3 minutes. OQ208 was used as the bandpass and flux density calibrator. The flux scale is accurate to $\sim 10\%$. The calibrated and edited Betelgeuse data

Table 2
Proper Motions for Betelgeuse^a

Reference	$\mu_{\alpha \cos \delta}$	$\sigma_{\mu_{\alpha \cos \delta}}$	μ_{δ}	$\sigma_{\mu_{\delta}}$
ESA (1997)	27.33	2.30	10.86	1.46
Boboltz et al. (2007)	23.98	1.04	10.07	1.15
Harper et al. (2008)	24.95	0.08	9.56	0.15
van Leeuwen (2007)	27.54	1.03	11.30	0.65
Radio-only ($\sigma_{\text{radio}}^{\text{noise}} = 2.4$ mas)	25.53	0.31	9.37	0.28

Note.

^a Units: mas yr⁻¹.

comprised 4–8 hr per antenna, spread over 10.5 hr, with an average bandwidth of 400 MHz. The data were imaged using two schemes, one for highest resolution and the other, with a slight tapering of the visibilities, for maximum sensitivity to the extended stellar atmosphere, using a 180 mas circular restoring beam. The latter was used to measure the astrometric position. The astrometric uncertainty arising from phase referencing is 16 mas, and adding the noise-based fitting uncertainty gives a total of 17.5 mas. Richards et al. (2013) describes these observations in more detail, but note that the measurements given in this paper are after re-processing using the correct receiver mount position for the Cambridge antenna (Beswick 2015).

Similar observations were made in 2015 March and June, but the phase reference 0605+0939 was used, $\sim 7^\circ$ from the target, giving a total astrometric uncertainty of 22.2 and 22.5 mas in March and June, respectively.

The total flux densities at successive epochs were 2.78, 2.39, and 2.35 mJy in areas 204×195 , 212×198 , and 201×189 mas², respectively, which is consistent with the barely significant ellipticity measured in VLA data. At all epochs, the high-resolution images (as reprocessed, for 2012) show different distributions of six to eight small hot spots at the level of $\approx 10\%$ of the total flux density. We tested whether these were biasing the fits by subtracting the hot spots from the 2012 visibility data and replacing them with the 2015 March hot spots, and re-imaging the modified 2012 data at 180 mas resolution. The position fitted was less than 1 mas different from the original measurement, suggesting that the hot spots seen at 5.75 GHz do not significantly bias the (tapered) measured e-MERLIN centroid position and thus are not a significant source of *Cosmic Noise* for this analysis.

2.3. Sources of Additional Radio Positional Noise

In Harper et al. (2008), the radio positions were assigned positional uncertainties under the assumption that the intensity weighted center was the position of the barycenter. However, the Lim et al. (1998) VLA Q-band (7 mm, 43 GHz) map shows the star is not axisymmetric, as it was better fit with a $95(\pm 2) \times 80(\pm 2)$ mas ellipse with a position angle (PA) of $67(\pm 7)$ deg (East of North). The presence of non-axisymmetric intensity distribution directly implies that one must consider the possibility of an offset between the weighted intensity centroid and the star’s barycenter. Elliptical fits have been made in subsequent multi-epoch multi-wavelength VLA maps (O’Gorman et al. 2015), and the orientation does not appear to reflect a fundamental property of the star, e.g., rotational distortion (Tatebe et al. 2007), and furthermore, the PA varies with time. For

example, an elliptical fit to the ALMA high-spatial resolution map (~ 330 GHz), which samples closer to the photosphere than the VLA Q-band, gives $54.50(\pm 0.01) \times 50.44(\pm 0.01)$ mas with a PA = $155.5(\pm 0.2)$ deg (O’Gorman et al. 2017).

The problem then is how do we quantify the magnitude of the intensity centroid shift with respect to the barycenter? At this point in time, nothing rigorous can be done because reliable grids of physically complete 3D atmospheric models describing this part of the atmosphere do not exist. Chiavassa et al. (2011) considered optical photo-center motions from radiative hydrodynamic simulations of a red supergiant like Betelgeuse that uses only gray opacities in the visible surface layers. They find a dispersion of 0.5 mas, which is consistent with ground-based interferometry obtained by Wilson et al. (1992; 0.4 mas) and Tuthill et al. (1997; 1.2 mas) but still smaller than the *Hipparcos Cosmic Noise* of 2.4 mas. More recently, Montargès et al. (2016) have presented H-band interferometry that reveals larger photo-center displacements at 4 epochs over 3 years with a mean displacement of 1.2 mas. Furthermore, during 2014, the photo-center moved by 3.4 mas. The H-band covers the $1.6 \mu\text{m}$ H⁻ opacity minimum and samples the deeper, more convective layers. SPHERE/ZIMPOL images from the VLT, with a resolution of ~ 20 mas, also reveal non-symmetric photospheric emission in the V ($\lambda 554$ nm; $\Delta\lambda = 81$ nm) and TiO717 filters ($\lambda 717$ nm; $\Delta\lambda = 20$ nm; Kervella et al. 2016). The global asymmetries observed with SPHERE/ZIMPOL can introduce apparent photo-center offsets of order ~ 1 mas.

For the high-spatial and high signal-to-noise ratio ALMA 2015 map, there are residuals to the uniform intensity ellipse fits. Eight different fits to the ALMA data, an ellipse with additional Gaussian spots, rings, and point sources, lead to shifts in the apparent ellipse centroid with a standard deviation of 0.43 mas. If we take these fits as possible realizations of radio-center displacements, then we can take 0.43 mas as a measure of the minimum of additional radio noise—that might correspond to the *Hipparcos Cosmic Noise*. However, the ratio of major to minor axis length of 1.1 suggests the potential for larger radio-center offsets. If we take the minor axis as representative of an unperturbed star, then there is a 5 mas extension for the other axis. We adopt approximately half this value as the nominal radio noise, i.e., $\sigma_{\text{radio}}^{\text{noise}} = 2.4$ mas. The similarity to the *Hipparcos Cosmic Noise* in the 2007 solution may be coincidental because the sensitivity of specific intensity to changes in gas temperature are much smaller on the Rayleigh–Jeans tail of the Planck function. Including this additional uncertainty in the radio positional errors (in quadrature) only has an effect on the few high-spatial resolution radio observations, which, apart from one, are from the VLA.

Simulations of optical photo-center displacement show timescales of months and years (Chiavassa et al. 2011), so the photo-center displacements are not random, as assumed in the *Hipparcos* astrometric fitting procedures. However, at this point there is little more that we can do except to point out a potential future solution in Section 6.1.

3. Radio-only Proper Motions and Parallax

It has already been noted that VLA radio positions suggest different proper motions to the 1997 *Hipparcos* astrometric solution (Boboltz et al. 2007; Harper et al. 2008; see Table 2). The differences become more significant now because the 2007

Table 3
Radio-only Astrometric Solutions^a

$\sigma_{\text{radio}}^{\text{noise}}$	π	σ_{π}	$\mu_{\alpha \cos \delta}$	$\sigma_{\mu_{\alpha \cos \delta}}$	μ_{δ}	$\sigma_{\mu_{\delta}}$
0.00 mas	3.33	1.93	25.77	0.28	9.55	0.24
0.43 mas	3.38	1.94	25.75	0.28	9.54	0.24
2.40 mas	3.77	2.20	25.53	0.31	9.37	0.28
4.80 mas	4.35	2.67	25.42	0.35	9.28	0.32
7.20 mas	5.16	3.11	25.37	0.37	9.26	0.35

Note.^a Units: mas for π , mas yr⁻¹ for μ .

Hipparcos solution has uncertainties that are a factor of >2 smaller.

Here, we consider the new radio data set and explore the proper motions and parallaxes that result from different levels of additional radio centroid noise. We compute the parallaxes using the JPL DE405 IRCF ephemerides (Standish 1998). These proper motions are presented in Table 3 where the uncertainties are calculated assuming the adopted astrometric model is the correct one. The parallaxes are not tightly constrained because there are only a few positions with small positional uncertainties comparable to the size of the parallax. The parallaxes are smaller than given by either the 1997 and 2007 *Hipparcos* solutions and the parallax increases with increasing radio *Cosmic Noise*. Considering Table 2, it can be seen that none of the proper motions ($\mu_{\alpha \cos \delta}$ or μ_{δ}) agree with the 2007 *Hipparcos* solution. This suggests that there is a bias in *Hipparcos* proper motions that may arise from too much weight being given to the direction 29° E. of N. The PA of Betelgeuse’s rotation axis, as deduced from combined UV spectral measurements, is $\sim 65^\circ$ E. of N. (Uitenbroek et al. 1998; Harper & Brown 2006), and with a period of ≥ 17 yr, equatorial motion of bright regions is unlikely to be an explanation. However, 1991–1992 interferometry from Wilson et al. (1992) and Tuthill et al. (1997) show hot spots that shift the photo-center with respect to the extended disk to PA’s of 39° (1991 January) and -29° (1992 January), which can be attributed to photospheric convective motions (Chiavassa et al. 2011). This provides evidence that photo-center motions did occur during the *Hipparcos* mission, and these may have contributed to the necessity of adopting a stochastic solution.

4. Revised Intermediate Astrometric Solutions

The HIAD were retrieved from the DVD included in van Leeuwen (2007, Appendix G2.1).⁹ There are 66 scan level abscissa (a) measurements, and we reject one outlier measurement, as in the 2007 published solution. This represents an increase in the number of measurements from the original reduction (38). van Leeuwen (2007, Equation (2.52)) gives the differences between predicted and measured abscissae (residuals, da) as

$$da = \cos \psi d\alpha \cos \delta + \sin \psi d\delta + \text{PARF } d\pi + \cos \psi \Delta t d\mu_{\alpha \cos \delta} + \sin \psi \Delta t d\mu_{\delta} \quad (1)$$

where π is the parallax and PARF (known as the parallax factor), ψ , is related to the scan angle. For each scan, the estimated abscissa uncertainties σ_a are also provided. For the stochastic solution, σ_a includes the additional *Cosmic Noise* of $\sigma_{\text{Hipp}}^{\text{noise}} = 2.4$ mas. The residuals from the van Leeuwen (2007)

⁹ There is a very small difference in some of the adopted astrometric values available on-line and on the DVD.

Table 4
Astrometric Solutions for Betelgeuse

Parameter	van Leeuwen (2007)	Present Work
$\Delta\alpha \cos \delta$ (mas)	0.00 (0.71)	0.09 (0.19)
$\Delta\delta$ (mas)	0.00 (0.58)	1.40 (0.48)
Parallax π (mas)	6.55 (0.83)	4.51 (0.80)
$\mu_{\alpha \cos \delta}$ (mas yr ⁻¹)	27.54 (1.03)	26.42 (0.25)
μ_{δ} (mas yr ⁻¹)	11.30 (0.65)	9.60 (0.12)

solution, da , PARF, ψ , and Δt are given in the DVD. The published solution represents the minimum of

$$\chi^2 = \sum_{i=1}^{65} \left(\frac{da}{\sigma_a} \right)^2. \quad (2)$$

Introducing information from the radio positions, e.g., proper motions, leads to perturbations about the 2007 *Hipparcos* solution, i.e., $d\alpha \cos \delta$, $d\delta$, $d\pi$, $d\mu_{\alpha \cos \delta}$, and $d\mu_{\delta}$, whose effect on the optimum solution can then be explored using Equations (1) and (2). Both the radio and 2007 *Hipparcos* solutions are given in the International Celestial Reference System (ICRS). The uncertainty in the link between the 1997 *Hipparcos* catalog (Perryman et al. 1997) and ICRS at J1991.25 was 25 mas yr⁻¹ in the relative motions of the frames, and the *Hipparcos* 2007 catalog is in agreement to within the uncertainties (van Leeuwen 2007, S3.6).

5. Results*5.1. Radio Fixed Proper Motions and HIAD*

The long time span of the radio observations provides a powerful constrain on the proper motions. By fixing $\mu_{\alpha \cos \delta}$ and μ_{δ} for the case of $\sigma_{\text{radio}}^{\text{noise}} = 2.4$ mas (Table 2) in Equations (1) and (2), we find a parallax of $\pi = 5.27 \pm 0.78$ mas. This gives a distance of 190_{-25}^{+33} pc, which is larger than the *Hipparcos* revised 2007 value of 152_{-17}^{+22} pc. Examination of the correlation coefficients of the 2007 *Hipparcos* solution shows that the parallax is positively correlated with both proper motions. The radio proper motions are both smaller than the 2007 *Hipparcos* solution so the parallax is also smaller, and the distance greater.

5.2. Radio Positions and HIAD

New astrometric solutions were then obtained using the revised HIAD combined with the full radio positional data in Table 1 and Harper et al. (2008, and references therein). We minimized the χ^2 from the residuals in Equations (1) and (2) combined with the radio position offsets ($d\alpha \cos \delta$ and $d\delta$) weighted by their uncertainties. We used Levenberg–Marquardt least-squares minimization (Markwardt et al. 2009) with the 65 1D HIAD scans and each of the 18 2D radio position. For the radio, the residuals in $d\alpha \cos \delta$ and $d\delta$ were evaluated separately, effectively giving 36 datum (2×18 positions), for a total of 101 individual evaluations. The result, assuming $\sigma_{\text{radio}}^{\text{noise}} = 2.4$ mas, is given in Table 4, along with the 2007 *Hipparcos* solution. For convenience, the position offsets for the 1991.25 Epoch are given with respect to the 2007 *Hipparcos* solution. Figure 1 (top) depicts this solution along with the radio positions, while the bottom panel shows the 2007 *Hipparcos* solution.

The most significant difference between the radio+*Hipparcos* and the 2007 *Hipparcos* solution is the proper motion in declination where the 2007 value of 11.32 ± 0.65 compares

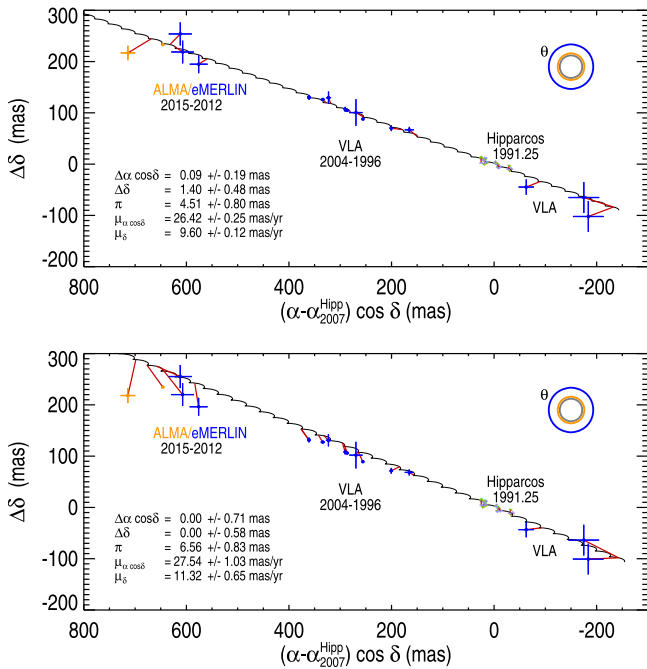


Figure 1. Top: the new astrometric solution computed with an assumed radio *Cosmic Noise* of 2.4 mas. The 1997 HIAD *Hipparcos* data are shown for illustration (see Harper et al. 2008). On this scale, the 1997 *Hipparcos* data are not distinguishable from the 2007 data. The apparent angular diameter of the star at different wavelengths is shown in the upper-right corner for reference—the inner circle is H-band (1.6 μm), the yellow is ALMA (338 GHz), and blue is Q-band (43 GHz). Bottom: the 2007 *Hipparcos* solution, which shows how the radio data constrains the proper motions. The radio data show that *Hipparcos* systematically overestimates μ_{δ} and, to a lesser extent, $\mu_{\alpha \cos \delta}$.

to 9.60 ± 0.12 mas yr $^{-1}$. This illustrates the importance of the long time span of the radio observations, and again hints that there is a preferred direction of the effective optical photo-center displacement during the *Hipparcos* observing epoch. Astrophysically, the most important result is that the combined radio+*Hipparcos* parallax is 4.51 ± 0.80 mas or 222_{-33}^{+48} pc, which is 0.7σ greater than that found by Harper et al. (2008). Both the solution using just the radio proper motions, and the combined radio+*Hipparcos*, lead to a smaller parallax and greater distance than either of the published *Hipparcos* results. Figure 2 shows the sensitivity of the new parallax to the adopted radio *Cosmic Noise*. Above 2.4 mas, the few precise radio positions lose their impact and the combined solution is controlled by the proper-motion constraints (which remain insensitive to the adopted value of $\sigma_{\text{radio}}^{\text{noise}}$). There is certainly an argument to be made that the parallax could be smaller by adopting a smaller $\sigma_{\text{radio}}^{\text{noise}}$ in the combined solution.

The tension between the optical (closer distance) and radio (farther distance) means that any changes in the relative weighting of the two data sets, either through the number of effective measurements or the additional added *Cosmic Noise*, will shift the parallax to some degree. However, these results show that *Hipparcos* still overestimates the parallax.

We note that Betelgeuse is very bright, too bright for *GAIA* to observe, and it is not clear that the small Japanese Nano-Jasmine 5.25 cm IR telescope satellite¹⁰ will be able to get useful data for Betelgeuse (if it is launched).

¹⁰ <https://directory.eoportal.org/web/eoportal/satellite-missions/n/nano-jasmine>

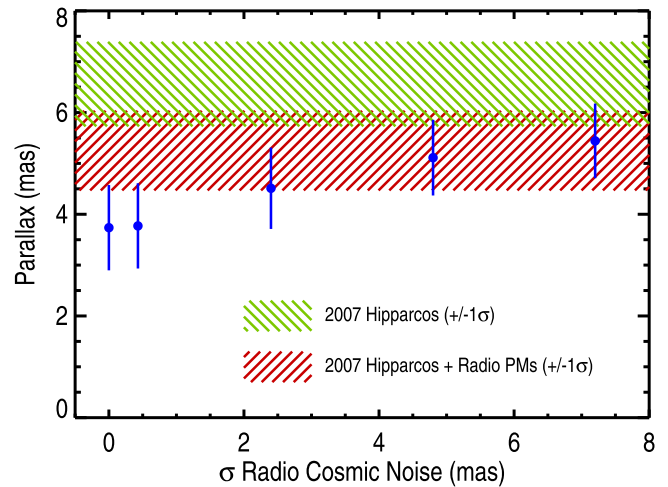


Figure 2. The parallax from the combined radio and 2007 *Hipparcos* HIAD data as a function of *Radio Cosmic Noise* ($\sigma_{\text{radio}}^{\text{noise}}$). The top hashed area (green) is the 2007 *Hipparcos* solution, and the hashed area below (red) is *Hipparcos* HIAD combined with the radio-only proper motions (this work, assuming $\sigma_{\text{radio}}^{\text{noise}} = 2.4$ mas). The combined radio+*Hipparcos* solutions are shown as circular symbols and error bars (blue) for different values of assumed $\sigma_{\text{radio}}^{\text{noise}}$. When $\sigma_{\text{radio}}^{\text{noise}} > 3$ mas, the sensitivity of the parallax to the radio positions is reduced.

6. Discussion

While the astrometric solutions presented above are probably the best that can be done at the present time, it is not the final solution to the problem of the stellar distance. The present parallax for Betelgeuse implies it is 1.2 times more luminous than in Harper et al. (2008), but the uncertainties remain significant for astrophysical purposes. To obtain a solid parallax measurement requires multiple observations where one could simultaneously measure the intensity position, with reference to accurate position (phase) calibrators, and image the uneven intensity distribution on the stellar surface. In this way, one has the chance that the continuum centroid and uncertainties from surface intensity variations could be estimated with sufficient precision to enable a reliable parallax determination.

6.1. What is the Optimum Wavelength to Make Astrometric Measurements?

The outer atmosphere of the convective M supergiant may be shaped by gas pressure, rotation, convective motions, shocks, and magnetic fields competing with the stellar gravitational field. These may lead to surface brightness variations that are not centered on the star's barycenter, which in turn will influence the astrometric solution. For Betelgeuse, rotation is not expected to lead to significant surface distortion (Tatebe et al. 2007). One would like to sample the layers well above the optically thin visual surface and where convection-induced height variations are minimized. Surface magnetic fields are expected to decrease more slowly with height than the gas density (pressure) and magnetic fields are expected to shape the outer layers (Harper 2013), including the hotter ultraviolet emitting chromospheric region near $2R_*$. When the gas temperature increase to above ~ 4000 K, hydrogen becomes a significant electron donor and the radio opacity can increase significantly. This suggests that an optimal radial location for astrometric measurements is well above the photosphere but interior to the higher temperature chromosphere. This region is still relatively uncharted and is expected to host low-temperature inhomogeneities related to the

MOLsphere phenomenon (Tsuji 2006; Ohnaka et al. 2009), which is probably the cooler and lower-gravity equivalent of the COMosphere phenomenon observed in warmer stars, including K giants and the Sun (Wiedemann et al. 1994; Ayres 2002).

The intensity changes (ΔI) resulting from differences in temperature (ΔT) in a given layer are expected to be less in the sub-mm and cm than in the optical because the thermal continuum emission is on the Rayleigh–Jeans tail where perturbations should be linear in temperature, i.e., $\Delta I \propto \Delta T$. In the optical, the sensitivity is greater because of the exponential nature of the Planck function, and in the V-band there is additional sensitivity resulting from the sensitivity of molecular opacity to temperature.

Fortunately, the mm and sub-mm radio frequencies probe the optimum atmospheric layers, and in addition, high-spatial resolution observations can image these layers at the same time as the position is accurately known with respect to an external reference frame (ICRS). This may be achieved with ALMA in the sub-mm, and perhaps in combination with the JVLA at Q-band (43 GHz, 6.9 mm). These observations would need maximum baseline configurations for the highest spatial resolution.

To obtain an accurate and precise parallax for Betelgeuse will require a dedicated multi-year observing plan. In addition to requiring good weather conditions for atmospheric phase stability, Betelgeuse observations with multiple check sources are needed near maximum parallax shift. Redundant observations will need to be planned because experience shows that data will be lost to bad weather. Another challenging constraint is that interferometer array configurations are routinely changed in non-yearly cycles to satisfy other science priorities.

7. Conclusions

The VLA+ 1997 *Hipparcos* HIAD astrometric solution for Betelgeuse (Harper et al. 2008) has been improved by using the revised 2007 *Hipparcos* HIAD from van Leeuwen (2007) combined with extant VLA data and new e-MERLIN and ALMA positions. The non-axisymmetric intensities found in high-spatial resolution VLA and ALMA radio maps indicate that the intensity centroid may not coincide with the barycenter, leading us to introduce radio *Cosmic Noise* analogous to that required for the *Hipparcos* optical solutions.

First, we find that using the proper motions from the radio data alone, which has a time span of 34 years, leads to a smaller parallax (greater distance) than either *Hipparcos* solution (time span of 28 months). Second, the new combined radio+*Hipparcos* astrometric solution gives a parallax and distance of 4.51 ± 0.80 mas and 222_{-34}^{+48} pc, respectively. This distance is slightly larger, but not significantly so, than the previous radio+*Hipparcos* solution of 197_{-35}^{+55} pc (Harper et al. 2008). However, the new solutions are 1.6σ and 2.6σ different from the 2007 *Hipparcos* solution of van Leeuwen (2007). To obtain a more precise parallax will require high-spatial resolution continuum observations in the mm and sub-mm that can be obtained with ALMA and JVLA. Scheduling and obtaining the required observations may take a Herculean effort.

Financial support for this work was provided by NASA through a SOFIA grant NAS2-97001 issued by USRA to G.M.H., who also acknowledges the assistance of R.W.H. P.K. acknowledges financial support from the Programme National de Physique

Stellaire (PNPS) of CNRS/INSU, France. E.O.G. acknowledges support from the Irish Research Council. L.D. acknowledges support from the ERC consolidator grant 646758 AEROSOL and the FWO Research Project grant G024112N. This paper makes use of the following ALMA data: ADS/JAO.ALMA#2015.1.00206.S. ALMA is a partnership of ESO (representing its member states), NSF (USA) and NINS (Japan), together with NRC (Canada), NSC and ASIAA (Taiwan), and KASI (Republic of Korea), in cooperation with the Republic of Chile. The Joint ALMA Observatory is operated by ESO, AUI/NRAO, and NAOJ. The National Radio Astronomy Observatory is a facility of the National Science Foundation operated under cooperative agreement by Associated Universities, Inc. This research has made use of the Vizier catalogue access tool, CDS, Strasbourg, France. It has also made use of NASA’s Astrophysics Data System Bibliographic Services. Finally, we thank the referee for their insights.

Facilities: *Hipparcos*, VLA, ALMA, e-MERLIN.

References

- Airapetian, V. S., Ofman, L., Robinson, R. D., Carpenter, K., & Davila, J. 2000, *ApJ*, 528, 965
- Ayres, T. R. 2002, *ApJ*, 575, 1104
- Beswick, R. 2015, Inclusion of an Axis-offset to Cambridge telescope data within e-MERLIN (June 9), e-MERLIN Technical Memo
- Boboltz, D. A., Fey, A. L., Puatua, W. K., et al. 2007, *AJ*, 133, 906
- Chiavassa, A., Pasquato, E., Jorissen, A., et al. 2011, *A&A*, 528, A120
- Dolan, M. M., Mathews, G. J., Lam, D. D., et al. 2016, *ApJ*, 819, 7
- ESA 1997, The *Hipparcos* and *Tycho* Catalogues, ESA, SP-1200
- Freytag, B., Steffen, M., & Dorch, B. 2002, *AN*, 323, 213
- Garrington, S., & Beswick, R. 2016, *A&G*, 57, 3.28
- Harper, G. M., & Brown, A. 2006, *ApJ*, 646, 1179
- Harper, G. M., Brown, A., & Guinan, E. F. 2008, *AJ*, 135, 1430
- Harper, G. M., DeWitt, C., Richter, M. J., et al. 2017, *ApJ*, 836, 22
- Harper, G. M. 2013, in *Betelgeuse Workshop 2012*, EAS Publications Ser. 60, ed. P. Kervella, T. Le Bertre, & G. Perrin (Les Ulis: EDP Sciences), 59
- Hartmann, L., & Avrett, E. H. 1984, *ApJ*, 284, 238
- Haubois, X., Perrin, G., Lacour, S., et al. 2009, *A&A*, 508, 923
- Kervella, P., Lagadec, E., Montargès, M., et al. 2016, *A&A*, 585, A28
- Lim, J., Carilli, C. L., White, S. M., Beasley, A. J., & Marson, R. G. 1998, *Natur*, 392, 575
- Markwardt, C. B. 2009, in *ASP Conf. Ser. 411, Astronomical Data Analysis Software and Systems XVIII*, ed. D. A. Bohlender, D. Durand, & P. Dowler (San Francisco, CA: ASP), 251
- Martí-Vidal, I., Vlemmings, W. H. T., Muller, S., & Casey, S. 2014, *A&A*, 563, A136
- Montargès, M., Kervella, P., Perrin, G., et al. 2016, *A&A*, 588, A130
- O’Gorman, E., Harper, G. M., Brown, A., et al. 2015, *A&A*, 580, A101
- O’Gorman, E., Kervella, P., Harper, G. M., et al. 2017, *A&A*, in press
- Ohnaka, K., Hofmann, K.-H., Benisty, M., et al. 2009, *A&A*, 503, 183
- Perryman, M. A. C., Lindegren, L., Kovalevsky, J., et al. 1997, *A&A*, 323, L49
- Richards, A. M. S., Davis, R. J., Decin, L., et al. 2013, *MNRAS*, 432, 61
- Smith, N., Hinkle, K. H., & Ryde, N. 2009, *AJ*, 137, 3558
- Standish, E. M. 1998, *JPL IOM*, 312. F-98 - 048
- Tatebe, K., Chandler, A. A., Wishnow, E. H., Hale, D. D. S., & Townes, C. H. 2007, *ApJL*, 670, L21
- Tsuji, T. 2006, *ApJ*, 645, 1448
- Tuthill, P. G., Haniff, C. A., & Baldwin, J. E. 1997, *MNRAS*, 285, 529
- Uitenbroek, H., Dupree, A. K., & Gilliland, R. L. 1998, *AJ*, 116, 2501
- van Leeuwen, F. (ed.) 2007, *Hipparcos, the New Reduction of the Raw Data: Astrophysics and Space Science Library* (Springer: Berlin), 350
- Wiedemann, G., Ayres, T. R., Jennings, D. E., & Saar, S. H. 1994, *ApJ*, 423, 806
- Wilson, R. W., Baldwin, J. E., Buscher, D. F., & Warner, P. J. 1992, *MNRAS*, 257, 369